Published in final edited form as:
J Clin Neurophysiol. 2010 August ; 27(4): 274–284. doi:10.1097/WNP.0b013e3181eaa9f5.

Mutual Information Analysis of EEG Signals Indicates Age-Related Changes in Cortical Interdependence during Sleep in Middle-aged vs. Elderly Women

Pravitha Ramanand, **Margaret C. Bruce**, and **Eugene N. Bruce**
Center for Biomedical Engineering, University of Kentucky, Lexington, KY 40506 U. S. A

Abstract

Elderly subjects exhibit declining sleep efficiency parameters with longer time spent awake at night and greater sleep fragmentation. In this paper, we report on the changes in cortical interdependence during sleep stages between 15 middle aged (range: 42-50 years) and 15 elderly (range: 71-86 years) women subjects. Cortical interdependence assessed from EEG signals typically exhibits increasing levels of correlation as human subjects progress from wake to deeper stages of sleep. EEG signals acquired from previously existing polysomnogram data sets were subjected to mutual information (MI) analysis to detect changes in information transmission associated with change in sleep stage and to understand how age affects the interdependence values. We observed a significant reduction in the interdependence between central EEG signals of elderly subjects in NREM and REM stage sleep in comparison to middle-aged subjects (age group effect: elderly vs. middle aged $p<0.001$, sleep stage effect: $p<0.001$, interaction effect between age group and sleep stage: $p=0.007$). A narrow band analysis revealed that the reduction in MI was present in delta, theta and sigma frequencies. These findings suggest that the lowered cortical interdependence in sleep of elderly subjects may indicate independently evolving dynamic neural activities at multiple cortical sites. The loss of synchronization between neural activities during sleep in the elderly may make these women more susceptible to localized disturbances that could lead to frequent arousals.

Keywords

Age; Sleep; Mutual Information; Interdependence

A. INTRODUCTION

The effects of physiological aging on sleep have been researched since the 1980s (Feinberg et al., 1984; Dijk et al., 1989; Ehlers and Kupfer, 1989). Most studies based on whole night hypnograms have found that the elderly spend more time awake and have lower sleep efficiency and greater sleep fragmentation. The elderly also spend less time in slow wave sleep (delta sleep). Delta power is reduced greatly with increasing age in the first NREM period of the night and delta power reduction over the later sleep epochs usually observed in

Pravitha Ramanand, Ph. D, Center for Biomedical Engineering, University of Kentucky, Lexington, KY 40506-0070 U. S. A., Tel: 859-323-3876, FAX: 859-257-1856, r.pravitha@uky.edu.

young subjects occurs to a much lesser extent in elderly subjects (Carrier et al., 2001). Major causes of sleep fragmentation in the elderly are multiple arousals attributed to extrinsic factors such as pain, apneas and other breathing-related disruptions (Smith and Haythornthwaite, 2004). There may also be neurodegenerative factors such as Alzheimer's disease that cause sleep disruption in the elderly. The changes in elderly sleep patterns may reflect age-related changes in the neuronal network activations or interconnections that produce and regulate normal sleep in humans. There may also be disrupting factors acting on the neural mechanisms causing alterations to the duration of sleep stages in the elderly. A better understanding of sleep dynamics in the healthy elderly may prove beneficial to clinicians in diagnosing and treating age-related sleep disorders.

Quantitative sleep studies have traditionally analyzed amplitude and spectral measures such as spectral power density and correlation (Armitage et al. 1992; Corsi Cabrera et. al., 2000; Ferrara et. al., 2002). These studies identified variations in the spectral band powers as sleep progressed from wake (W) to stages 1-4 (NREM) and REM. On the other hand, the origin of the waves that compositely form the sleep EEG was explored from a cellular and neural oscillations standpoint by Steriade and others (Achermann and Borbély, 1997; Steriade 1999). The predominance of delta waves in sleep led to close investigation of the low frequency, high amplitude oscillations in animal and human sleep patterns at macroscopic as well as neuronal levels. Lately, the unique characteristics of the <1 Hz delta oscillation has captured the attention of sleep researchers. It is suggested that the low frequency component of delta may have a functional role different from that of 1-4 Hz delta rhythm during sleep (Campbell et al., 2006) and may synchronize spatially distributed neural activities during specific periods of NREM sleep (Ferri et al., 2005). Furthermore, low frequency delta power does not decline over successive NREM sleep periods, and it has a cortical origin in contrast to the thalamocortically-generated high frequency delta rhythm (Achermann and Borbély, 1997; Steriade and Amzica, 1998). The functional correlates of alpha rhythms during wake and sleep stages have also been reevaluated following research that suggested the existence of different sites of generation and non-uniform topographic scalp distribution for this spectral component (Pivik and Harman, 1995; Cantero et al., 2002).

In recent times, the application of methods derived from the theory of dynamical systems has supplemented the frequency content based analysis of sleep EEG. Measures such as generalized dimensions and Lyapunov exponents have been used to characterize the static and dynamic properties of the neurophysiological system generating the EEG signal (Fell et al., 1996; Pereda et al., 1999; Kobayashi et al., 2001; Acharya et al., 2005). The differences in features such as irregularity and long range correlations of EEG signals in various sleep stages between healthy people and patients with sleep-disordered breathing are the topic of many publications (Lee et al., 2004; Burioka et al., 2005). In light of findings from multiple studies, it is widely accepted that stages 3 and 4 of sleep, known as slow wave sleep (SWS), are characterized by high delta band powers and corresponding lowered dynamical complexity.

Multivariate measures have been applied to assess the interdependence of cortical regions during sleep. The interdependence between EEG signals depends on the functional differentiation of cortical regions. This implies that differences in activation of the cortical regions can cause individual dynamics at these sites to evolve almost independently of each other resulting in low correlation between them. Studies on EEG signals from healthy, young subjects using spectrally based coherence measures and other nonlinear interdependence measures have reported higher coherence between cortical regions during deeper sleep stages (Guevara et. al., 1995, Achermann and Borbély, 1998, Pereda et al., 2001). In normal sleep, large responses to localized disturbances are attenuated by the high coupling between cortical sites. A lowered interdependence in sleep may increase the

likelihood of such responses persisting and reaching levels usually associated with active awake states, causing arousals or awakenings to the detriment of sleep continuity. Thus, decreased inter-regional correlation during sleep may explain some aspects of declining sleep quality in the elderly population. Previous reports about age-related differences in the spectral analysis of sleep stages suggests that the behavior of cortical interdependence of aging subjects may indeed be different from that of young subjects during sleep (Carrier et al., 2001; Darchia et al., 2007). Our objective in this study was to assess the cortical interdependence across cortical regions during sleep in healthy adults by analyzing the scalp EEG signals.

Different measures of connectivity between physiological signals have been introduced and applied extensively to assess the interdependence between brain regions under different conditions (David et al., 2004; Pereda et. al., 2005). The Mutual Information (MI) derived from information theory is one such measure which assesses the amount of information about one signal contained in another signal (Fraser and Swinney, 1986). Hence, when applied to two EEG signals, MI gives a measure of dynamical coupling between them. In comparison to other connectivity measures, mutual information is a measure of statistical dependence between signals that does not make an assumption on the nature (whether linear or otherwise) of the generating system of the signals and gives stable estimates with reasonably long data sets. MI can also be useful in narrow band analyses to determine the information content of the different spectral bands in the EEG (David et al., 2004). Narrow band coupling may be dependent on age and gender as well as on sleep stage. When the MI is extracted from a single signal, it is called the auto mutual information (AMI). The AMI quantifies the linear and nonlinear correlations contained in the signal as a function of elapsed time between observations. MI has been applied to the human EEG in different contexts.

An early application of the MI to single channel signals determined the characteristic time at which the auto mutual information reached a minimum as a measure of the time delay utilized in delay embedding methods for system characterization (Fraser and Swinney, 1986). To study the information transfer across brain regions, MI was applied to EEGs from normal subjects and from subjects suffering various pathological conditions (Jeong et al. 2001; Na et al. 2002). Patients suffering from conditions such as Alzheimer's disease were found to exhibit lowered information transmission, especially across anterior-posterior brain regions. Na and coworkers (2006) applied MI analysis to study the effects of total sleep deprivation on waking human EEG. This study revealed lower MI following sleep deprivation between the left central and frontal brain areas, implicating homeostatic deterioration in these regions. Xu et al. (1997) analyzed sleep EEG from young subjects using MI to demonstrate higher values of information transmission in deeper stages of sleep.

In the present paper, we applied the MI method to EEG segments chosen from undisturbed sleep stages of elderly (age range- 71-86 years) and middle aged subjects (age range- 42-50 years) to explore the inherent differences in the information content of the signals. By undisturbed we mean EEG sleep stage epochs uninterrupted by events such as hypopneas, apneas and arousals. Analysis was carried out on broad as well as narrow band EEG to investigate if the EEG interdependence changed within spectral bands in different sleep stages. As sleep progresses from W to SWS, the delta band oscillations increasingly dominate the EEG. Therefore, we hypothesized that age-related effects may arise in this band. The proposed significance of the slow component of the delta band also prompted us to further divide the traditional delta band of EEG frequencies up to 4 Hz into a low delta, (Delta_L: 0.2-2 Hz) band and a high delta (Delta_H: 2-4 Hz) band to better resolve the changes occurring within the delta band.

B. METHODS

1. Subjects and EEG recordings

Mutual Information analysis was conducted retrospectively on overnight polysomnogram (PSG) EEG datasets obtained from the NIH-sponsored Sleep Heart Health Study (SHHS) (Quan et al., 1997). Fifteen healthy middle-aged (MA) Caucasian women of mean age 46.93 ± 1.91 yrs (range: 42-50 yrs), and fifteen healthy elderly (ELD) Caucasian women of mean age 77.8 ±4.20 (range: 71-86 yrs) were selected for this study. These subjects did not have sleep-disordered breathing or a history of stroke and were not taking any medications known to interfere with sleep. The Respiratory Distress Index (5% RDI) for the elderly group was 1.99±1.56 (range: 0 −5.10) and for the middle aged subjects, 1.6±2.13 (range: 0-5.28).

The overnight PSG studies were conducted in the SHHS participants' homes by certified technicians (Redline et al., 2004). The PSG data recorded for each subject included: EEG leads C3A2 and C4A1, a right and a left electro-oculogram (EOG), a bipolar submental electromyogram (EMG), electrocardiogram (EKG), nasal airflow, respiratory excursions of the thorax and abdomen, and finger pulse oximetry. The EEG was acquired at a sampling rate of 125 Hz. A notch filter at the 60 Hz electrical mains contamination was designed and applied to the EEG signals. Sleep staging was scored by SHHS personnel at 30 s intervals based on the Rechtschaffen and Kales (R&K) criteria (Rechtschaffen and Kales, 1968). For each subject, we selected six 30 s segments of EEG data from Wake, stages 2 and 3 of NREM, and REM during the first sleep epoch (90 segments per group per stage). Due to the lack of sufficient segments from stages 1 and 4 of NREM sleep, especially for the elderly subjects, these stages were not analyzed. EEG segments that were scored as free from respiratory or movement artifacts were selected. Also, the chosen sleep segments did not include disruptive events such as apneas, hypopnias or arousals. For the narrow band analyses, the EEG signals were band pass filtered using a bank of fourth order elliptic filters with peak to peak ripple of 1 dB and stop band attenuation of 40 dB. The EEG signal was filtered into the following bands: low delta (Delta_L): 0.2 to 2 Hz, high delta (Delta_H): 2 to 4 Hz, theta: 4 to 8 Hz, alpha: 8 to 12 Hz, sigma: 12 to 16 Hz, and beta: 16 to 24 Hz.

2. Mutual Information (MI)

Mutual Information, a metric derived from information theory, quantifies the information gained about one random event from observations of another (Fraser & Swinney, 1986). It measures the linear and nonlinear dependencies that may exist between two sets of data. Hence, MI is often regarded as the nonlinear counterpart of the correlation function which identifies linear dependencies between two data series (Abarbanel et al., 1993, Cellucci et al., 2005). The MI function can be applied to two time series as a cross measure of mutual information (CMI), and when applied to a single data series it is referred to as the Auto Mutual Information (AMI).

Consider $X = \{x_i\}$ and $Y = \{y_j\}$ representing two sets of random observations with probability distribution of amplitudes given by $P_X(x_i)$ and $P_Y(y_j)$, respectively. The average amount of information gained from measurements of X is obtained from Shannon information theory as

$$H(X) = -\sum_{x_i} P_X(x_i) \log P_X(x_i) \quad (1)$$

This is the a priori uncertainty in X existing before any measurements are made. The conditional uncertainty in a measurement of X, given that y_j is the measurement made in Y,

is $H(X \mid Y = y_j)$. The mean conditional uncertainty in measuring X under the condition that Y is known is then

$$H(X|Y) = \sum_{y_j} P_Y(y_j)\, H(X|Y=y_j) = -\sum_{x_i,y_j} P_{XY}(x_i,y_j) \log\left(\frac{P_{XY}(x_i,y_j)}{P_Y(y_j)}\right) = H(X,Y) - H(Y) \tag{2}$$

where, $H(X,Y) = -\sum_{x_i,y_j} P_{XY}(x_i,y_j) \log\left[P_{XY}(x_i,y_j)\right]$ The mutual information (MI) estimates the information gained about one signal by measuring the other. In other words, it quantifies the reduction in uncertainty of X by measurements made on Y and is given as

$$MI(X,Y) = H(X) - H(X|Y) = H(X) + H(Y) - H(X,Y) \tag{3}$$

From equations (1) and (2), the Cross Mutual Information between X and Y can be written as

$$CMI(X,Y) = \sum_{x_i,y_j} P_{XY}(x_i,y_j) \log\left(\frac{P_{XY}(x_i,y_j)}{P_X(x_i)\, P_Y(y_j)}\right) \tag{4}$$

Usually, the base of the logarithm in the above relations is 2 and information is then expressed in units of bits. By estimating the CMI for signals lagged in time, the CMI function can be obtained as a function of the time lag between them. This function gives the average number of bits of X that can be predicted by making measurements of Y. In a similar way, the Auto Mutual Information (AMI) function says how many bits on average about a given signal may be predicted by measurements on the time advanced version of itself.

The AMI between $X(t) = \{x_i\}$ and $X(t+\tau) = \{x_{i+\tau}\}$ is

$$AMI(X(t), X(t+\tau)) = \sum_{x_t, x_{t+\tau}} P_{XX_\tau}(x(t), x(t+\tau)) \log\left(\frac{P_{XX_\tau}(x(t), x(t+\tau))}{P_X(x(t))\, P_{X_\tau}(x(t+\tau))}\right) \tag{5}$$

The estimation of the probability functions in (4) and (5) pose a hurdle in estimating the MI function from time series data. While other estimators based on the nearest neighbor and kernel based methods exist (Papana and Kugiumtzis, 2008), the histogram based estimation was found to provide stable CMI functions and was used in this study. The average CMI computed over −0.2 s to 0.2 s was used as a measure of the interdependence between the signals. In the case of AMI, the rate at which information decays with time is an inverse measure of the predictability of the signal. Higher rate of decay is associated with a quicker loss of predictability of the signal (Abásolo et al., 2008). The behavior of the AMI curve prompted us to fit it with an exponential function of the form,

$$AMI(t) = c_0 + c_1 e^{-\lambda t} \cos^2(2\pi f_c t) \tag{6}$$

where λ is the decay rate and f_c is the central frequency of the band. The damped squared cosine equation for MI function is a natural generalization of the damped cosine model for

the autocorrelation function of signals. In the case of the broad band data where effects from all the spectral bands are present, the AMI curve was fit using,

$$AMI(t) = c_0 + c_1 e^{-\lambda t} \quad \text{with} \quad \cos^2(2\pi f_c t) = 1 \tag{7}$$

With this definition, we may say the central frequency for the unfiltered segment is the sampling frequency *f*s. The AMI curves of specific spectral bands did not exhibit much difference between sleep stages over short time lags. Hence, the estimated decay rates of AMI function for the different bands did not vary substantially. However, the small persistent changes in AMI at longer lag times in specific spectral bands are captured well by the average AMI parameter.

3. Surrogate analysis

The MI quantifies the linear and nonlinear correlations in the signal. The question of whether the estimated CMI detects dependencies other than linear ones between the sleep EEG signals is answered by applying the method of surrogate data (Theiler et al., 1992; Schreiber and Schmitz; 2000). Although the MI between independent signals is zero, the finite size of a data set often causes this lower bound to be greater than zero. The methodology we followed to establish the significance of the CMI values is similar to that of Pereda and coworkers (2001). In this two step procedure, first univariate surrogates, S^1, that contained the linear behavior of one of the signals, say E^1, were generated by the iterated Amplitude Adjusted Fourier Transform (iAAFT) method. The CMI of these with the other EEG signal, E^2, was computed. In case of true interdependence between E^1 and E^2 , *MI* (E^1 , E^2)will be always greater than *MI* (S^1 , E^2), because the surrogates are in no way correlated with E^2. For the pairs of signals for which interdependence was thus established, bivariate surrogates, $(S_2)^1$ and $(S_2)^2$, that preserved the linear properties of each of the signals and also the linear cross correlation between them, were generated by the iAAFT method for the multivariate case. If the signals have nonlinear correlations between them, then the MI of the original signals will be greater than that of the surrogates. This difference was detected using a rank order test at a pre-specified significance level, $(1-\alpha)\times 100\%$. For the one-sided tests in both the univariate and bi-variate cases, we generated $M = \left(\frac{1}{\alpha} - 1\right)$ surrogates. Including the original EEG segments, this gave an ensemble of $\left(\frac{1}{\alpha}\right)$ data sets. The probability that the observed CMI between the EEG signals is the largest in the ensemble of MI values due to chance is then exactly α. With $\alpha = 0.05$, the significance level was 95% and M= 19 surrogate sets were generated for the analysis in both cases. Because here the MI is computed as a function of time lag between the signals, in the final step we required that the estimated MI for the EEG signals be greater than that for the surrogates for at least 50% of the time lags considered. This condition ensured that the higher values of MI due to the interdependence between the signals that is present at short time lags is included in assessing the nature of the interdependence.

4. Statistical analysis

The statistical procedure was aimed at detecting significant variations in the MI parameters due to the age effect and the sleep stages in broad band and narrow band analyses. A mixed linear model implemented using SAS 9.1 software (SAS Institute Inc., Cary, NC) with an unstructured covariate design was applied to the estimated MI parameters. We specified the between subject factor AGEGROUP with two levels (ELD, MA) and the repeated measures within subject factor STAGE with 4 levels namely, W, S2, S3 and REM. The SUBJECT

factor was nested under AGEGROUP. A post hoc test based on the differences of least squares means was applied to identify significant differences in the main effects or in the AGEGROUP*STAGE term.

C. RESULTS

1. Cross mutual information analysis

CMI was calculated for the C3A2 and C4A1 EEG signals of 30 s duration from specific sleep stages from the two subject groups. Here and elsewhere, we used 13 bins to estimate the histograms involved in MI computation. In a recent paper on the AMI estimation of biomedical signals, Escudero et al. (2009) observed that the computation of MI is biased only when the binning used in histogram estimation is either too fine or too coarse. The reasons for analyzing 30 s windows are twofold. The sleep stage scoring is done over epochs of 30 s and we wanted the results to reflect the changes that occurred in the same time period. Also we ensured that nonstationarity did not affect the analysis significantly by comparing the MI functions over smaller window lengths with the MI functions from the whole data length. As mentioned earlier, spectral power variations across sleep stages of different bands exhibit an age effect. This may be manifested in the coupling behavior of spectral bands as well, and these effects may go undetected in a broad band analysis. Therefore, we carried out MI estimation over EEG signals filtered into the spectral bands, i.e., delta, theta, alpha, sigma and beta. The predominance of low frequencies during sleep states and the significance of the very low frequency (<1 Hz) delta rhythm stressed earlier, prompted us to divide the delta band into two regions and explore MI changes further within this band.

Figure 1 gives typical CMI functions between C3A2 and the time delayed C4A1 signal for the various sleep stages in a middle aged subject for both the broad band and the narrow band data as defined above. CMI between the central regions was low during wake as compared to the subsequent sleep stages of S2, S3 and REM. This behavior was observed for the broadband CMI and for most of the spectral regions as well. The beta band CMI values were in the range of 0.02-0.05. These values were compared with CMI values obtained for time shuffled surrogates of the data, which are equivalent to independent signals with all correlations removed. Because the CMI estimates for the beta band fell within the distribution of the CMI values for the IID surrogates, especially in the sleep (S2, S3 and REM) EEG segments, the beta band was not considered for further analysis. Mutual information function is nonsymmetrical about the time axis, and this behavior was taken into account by computing a measure for the CMI averaged over time. The averaged CMI (A-CMI) between the signals was computed over time delays of −0.2 to 0.2 s. In the broad band case, the averaged CMI between the signals increased from W, reached a maximum at S3, and then decreased in the REM state for both ELD and MA subjects. The broad band CMI contains an overall effect of the dominant spectral bands in a particular sleep stage. Figure 2(a) represents the estimated Mean ± Standard Error (S.E.) of the A-CMI for the ELD and MA subjects. It was observed that the ELD subjects had lower CMI values in all sleep states than the MA subjects. The mixed linear model analysis with AGEGROUP as a between-subjects factor with 2 levels and sleepstage (STAGE) as a repeated measure with 4 levels applied to the A-CMI values produced significant main and interaction effects (AGEGROUP: $F(1,28)=46.49$, $p<0.0001$; STAGE: $F(3,28)=63.59$, $p<0.0001$; AGEGROUP*STAGE: $F(3,28)=5$, $p=0.007$). The post hoc tests based on the mean differences of A-CMI revealed significantly lower values of CMI for the ELD group in S2, S3 and REM sleep stages when compared to MA subjects. The CMI difference in W was non-significant.

The narrow band CMI analyses yielded functions with characteristic frequencies close to twice the central band frequencies as observed in Figure 1. For instance, the Delta_H band defined over 2 to 4 Hz had CMI functions with a periodicity of approximately 6 Hz at low values of delay. The CMI functions for the bands (with the exception of beta band) are plotted in Figure 1 for each of the sleep stages. The low frequency bands especially delta, exhibited the largest CMI values among all spectral components not only in S2 and S3 stages but also in REM. Among the higher frequencies, the alpha band CMI for the W and REM states was higher than that for sigma band while the sigma band predominated in the NREM sleep stages of S2 and S3. Average CMI calculation was carried out on the narrow band signals and results of the statistical analysis are presented in Figure 3. For the sake of completeness, the estimated A-CMI values for the beta band are also presented. The statistical analysis had significant main and (AGEGROUP*STAGE) interaction effects for all bands except the alpha band for which only main effects were present. It is readily apparent that in most spectral bands, the interdependence between the signals was higher for the MA group than for ELD subjects during sleep states. Moreover, the higher spectral powers of low frequencies in the slow wave sleep stage had led us to expect higher interdependence in these bands in the S3 stage in comparison to that in S2. But contrary to expectation, the lower spectral bands (delta and theta) had higher CMI in S2 than in S3 while faster bands exhibited higher CMI in S3 than in S2. The MA subjects had significantly higher CMI in S2 state than in W state for Delta_H, theta and sigma bands in post-hoc comparisons (Delta_H: t-value=7.92, $p<0.001$; Theta: t-value=2.67, $p=0.01$; Sigma: t-value =9.13, $p<0.0001$). Such large variations between CMI values of W and S2 states were not observed for the ELD group.

2. Auto mutual information analysis

The AMI function quantifies the dependence of a signal on its time lagged self. The rate of decrease of AMI describes how quickly information regarding the signal is lost and is inversely related to its predictability. The AMI estimation of both C3A2 and C4A1 signals was carried out, but since the results of the statistical analysis were very similar in both signals, only results from the C3A2 signal are reported here. Figure 4 presents AMI functions normalized by the maximum value (at $\tau = 0$) for the C3A2 signal from a middle aged subject for broad band and narrow band data. While the broad band EEG exhibited variations between sleep stages in the rate of loss of AMI at low delays, this was not the case for the narrow spectral range AMI functions. Hence, in the broad band case, the rate of loss of AMI was quantified by a fit to the AMI function with a damped squared cosine function as in equations 6 and 7. The constants C_0 and C_1 were found to be of the order of 0.01 and 1.00, respectively. The decay rate, λ , estimated in each case was assessed for differences due to state and age difference between the two subject groups. The changes in AMI were more apparent at longer lag values for bands such as Delta_L, Delta_H and alpha. For the narrow band case, we computed the average AMI over a period of −0.2 to 0.2 s as a measure of the dependence inherent in the signal. These values were separately subjected to a statistical analysis identical to that in the CMI case.

The estimates of the decay rate obtained from the fit to the AMI function of the broad band signal are given in Figure 2(b). The decay rates in the different stages were nearly equal for the two subject groups especially in the W, S2 and S3 states. The statistical analysis demonstrated a significant difference due to the STAGE effect ($F(3,28) = 165.21$, $p<0.0001$) and the (AGEGROUP*STAGE) effect ($F(3,28) = 3.12$, $p = 0.042$). The post-hoc comparisons for the (AGEGROUP*STAGE) effect yielded significance for the REM state (t-value = 2.02, $p = 0.05$) alone. This indicated a significantly higher AMI decay rate for the ELD subjects than for the MA group in the REM state. The results of the post hoc comparisons for the significant STAGE effect are summarized in Figure 2(b). We observed

that the decay rate showed large variations with sleep stage, decreasing from the W to S3 state and then increasing to a level lower than W in REM. All states had significant pair-wise changes in the estimated decay rate. Since the decay rate is an inverse measure of the predictability, it followed that the signal predictability was lowest in the W state and highest in the S3 state. Between the intermediate decay rates exhibited by S2 and REM states, REM had a higher decay rate or lower predictability than the S2 state. The A-AMI measure computed for the broad band data exhibited very close values for the ELD and MA groups. The mean AMI was highest in the S3 state and lowest in the W state. In the broad band case, because they are both normalized measures, the A-AMI and decay rate of AMI function are inversely related. A faster loss of AMI means a quickly decaying function from the maximum value of 1.0 leading to a lower A-AMI measure in the same segment. The STAGE effect was the only significant effect from the statistical analysis ($F(3,28)=110.79$, $p<0.0001$). The post-hoc tests revealed all pair-wise comparisons between sleep stages to be significant as in the case of the decay rate. The A-AMI measure for the broad band is presented in Figure 2(c).

The A-AMI values obtained for each of the spectral bands were subjected to the statistical analysis to identify the significant effects of age, stage, and interactions therein, on the AMI. These results are summarized with the estimated means for the A-AMI measure in Figure 5. The low delta band had significant main effects of AGEGROUP ($F(1, 28) = 10.37$, $p= 0.0032$) and STAGE ($F(3,28)=17.05$, $p<0.0001$). Interestingly, the low delta AMI was higher for ELD than for MA subjects for all stages. In the Delta_H band, the S2 stage had significantly higher AMI than all others and for the theta band, S2 was higher than W and S3. The AGEGROUP*STAGE effect was just significant for the alpha band ($F (3, 28) =2.87$, $p=0.054$) and the S3 stage showed higher AMI for the ELD subjects than for the MA group (t-value=2.23, $p=0.03$). The sigma band also had significant AGEGROUP*STAGE effect ($F(3,28)=3.97$, $p=0.018$) and post hoc comparison identified higher A-AMI for the MA group in the S2 and S3 stages than for the elderly subjects. The beta band A-AMI had no significant main or interaction effects.

3. Significance tests using surrogate signals

The CMI measure of sleep EEG was tested using surrogate analysis to evaluate if the detected interdependence could be completely explained by the linear correlations of the data. Surrogate signals were derived from the EEG signals by preserving the linear characteristic contained in the power spectrum and/or the signal distribution. If linear dependencies did not fully account for the CMI between the actual EEG signals, the parameter computed from the EEG would have a value higher than that from the surrogates. The test was carried out in two steps following the procedure described in Methods section 3. A one-sided rank test applied to the CMI values estimated for the signals and the bi-variate surrogates in the second step of the analysis helped to reveal the nature of the interdependence. For nonlinear nature of interdependence to be present between segments, we stipulated that the mean CMI for the EEG signals be higher than that for all of the pairs of surrogates, and that the individual CMI values at discrete time steps be higher for the EEG signals in at least 50% of the time steps considered. In this manner, the higher MI values observed at short time lags between the EEG signals were taken into consideration. At longer lags, as the signals became more independent, the difference between MI values between the surrogates and signals was smaller. With this condition, we detected about 62% of S2 and 38% S3 segments in the MA group exhibiting interdependence values that could not be explained by linear correlations contained in the surrogates. For the ELD, significant NREM segments were 59% (S2) and 28% (S3) respectively. The wake segments with a nonlinear component in the CMI were ~ 22% for both age groups. In the case of REM, the ELD had 33% and the MA had 30% of the CMI values significantly higher than that for the

bivariate surrogate pairs. The NREM S2 state had the maximum number of nonlinear segments in both groups. However the segments with CMI values that failed to achieve significance based on independence between the segments was higher for the ELD group (14% as opposed to 5% in the MA).

D. DISCUSSION

In this study, we observed that elderly subjects exhibited lowered cortical interdependence during NREM and REM sleep stages in comparison to middle aged subjects. The narrow band CMI analysis identified the delta, theta and sigma bands as exhibiting these differences between the two subjects groups. While the signal predictability assessed from the decay rate of the AMI function was almost the same for the W, S2 and S3 states for both groups, the REM state of the elderly was characterized by greater signal unpredictability. The sigma band signal, however, had significantly greater information content in the NREM stages of MA subjects than for the elderly.

The mutual information measure was used in the present analysis to compare information transmission across cortical regions in different sleep stages between the middle aged and elderly subjects. The MI applied between two random signals will be theoretically zero when the two signals are completely independent of each other and, hence, reflects the coupling existing between the two signals. As a nonlinear counterpart of the auto correlation function, the AMI from single channel EEG was also studied to understand how the time dependence inherent in a signal varied across sleep stages. A higher AMI value would mean that with respect to a given instant, the signal continued to evolve in the same manner that it did a certain (probably short) time period before the instant and this would make it more predictable in time. The AMI of cortical EEG signals thus reflects the predictability inherent in the signal. A quickly decaying AMI function points to a less predictable signal that may cause a reduction in the information transmission between signals. Since neural origins of the individual spectral components of the EEG differ, the dynamical behavior exhibited in the different frequency bands may also be different. We attempted to find changes in CMI and AMI of signals from broad band and narrow band EEG so that the role played by specific neurophysiological mechanisms associated with the various EEG spectral components during different sleep stages can be understood further. While it is generally accepted that sleep parameters such as sleep efficiency and NREM sleep duration decline with age, we were interested in determining whether there are age-related changes in the interdependence of EEG activities of typical sleep stages devoid of confounding effects such as apneas, arousals etc. If so, such changes may contribute to macroscopic effects of declining sleep efficiency parameters seen in whole night hypnograms of elderly subjects. Since elderly subjects have characteristic differences in the EEG power of traditional bands such as delta during sleep stages when compared to young subjects, the narrow band analysis was expected to help in determining the frequency-specific nature of cortical interdependence. Multiple reports have indicated that aging in men is associated with an increase in sleep disordered breathing affecting sleep efficiency and architecture to a greater extent than women (Lin et al., 2008 and references therein). Hence it may be advantageous to seek changes in measures such as regional interdependence from healthy women on whom the impact of aging on sleep may be smaller.

During sleep, the information transmission in the central cortical regions from ELD subjects was significantly lower than that from MA subjects. The lowered CMI meant that local differences in EEG activity of ELD subjects may not be attenuated to the same extent as in MA subjects during sleep. This difference may be due to one of two mechanisms. On the one hand, there could be a dissociation between underlying cortical regions (such as cortical and sub-cortical structures). Alternatively, this could reflect a reduction in the strength of a

common drive to the neural circuits that was inducing the characteristic high interdependence values during sleep states. In either case, the result is that the EEG activities at the two sites become more independent with increasing age. This independence might mean less spatial uniformity of cortical sleep state in the ELD group. Some researchers support the theory that sleep states are linked to continuous levels of intensity or depth, rather than to discrete levels (Pardey et al., 1996). If so, lack of spatial homogeneity may mean that some cortical sites are more sensitive to disturbances or arousal stimuli during a given sleep stage and their localized activity in the faster spectral range may result in frequent arousals from sleep.

The average CMI parameter exhibited an increasing trend from wake state to deeper sleep states such as S2 and S3, and then decreased again in REM stage to a value above that of the wake state. This was in agreement with a sleep EEG study by Pereda and colleagues (2001) on young adults which reported higher nonlinear interdependence between signals in deeper sleep stages compared to awake resting states. From the narrow band analysis, we found that all bands exhibited higher CMI during NREM sleep states than during W. This also matched with results from an EEG analysis in which spectral band correlations increased during slow wave sleep when compared to waking levels (Guevara et al., 1995). However EEG sleep dynamics are known to exhibit both linear and nonlinear structures (Pereda et al, 1999). Hence, the interdependence quantified by the CMI function ensured that nonlinear dependencies between the signals were taken into account.

The interdependence between spectral components was further explored by narrow band CMI estimation. We found that the higher CMI computed from the broad band data in sleep stages had contributions not only from high interdependence of slow delta and theta band components but also from the faster alpha and sigma components. The low and high delta, theta and sigma components of EEG had lower CMI in ELD subjects during sleep stages of S2, S3 and REM in comparison to the MA group. The coherence peaks in the spindle frequency range (12-16 Hz) in S2 stage are well documented (Achermann and Borbély, 1998). The authors of that publication suggested that some waking information is carried by these frequencies during sleep that is relevant to specific functional process in sleep. If this information is of importance in sleep, then reduced high frequency CMI in sleep may be a key factor affecting the decline of macroscopic sleep quality parameters of elderly subjects.

The decay rate of auto mutual information decreased from W to S2 to S3, and then increased in REM stage for the broad band EEG data. The AMI decay rate quantifies how quickly information about a signal is lost as a function of time delay. The decay rate of AMI is thus an inverse measure of the regularity or predictability of the signal. This can be understood as a variation in the EEG spectral content as sleep progresses from the wake condition. The faster spectral bands become less dominant as sleep deepens to S3 and the synchronous delta range frequencies exhibit greater regularity or a slower rate of decay of predictability. The faster alpha and/or beta waves reemerge in the REM state exhibiting stronger power and causing a faster loss of information in REM. In a study of the regularity aspect of sleep EEG, we reported enhanced regularity in deeper sleep stages as compared to wake and REM (Bruce et al., 2009). This analysis reaffirms the findings of that study by showing significant differences in the pair-wise comparison of decay rates between all stages. Moreover, the ELD group AMI decay rate in REM was higher than that of the MA group, indicating lower predictability of EEG in this state for the ELD subjects. These findings are consistent with the reported loss of regularity (i.e., increased Sample Entropy) of the elderly in REM in our previous study.

The narrow band analysis presents a more detailed picture of the self-dependence of EEG signals in sleep. Both subject groups exhibited higher AMI values in the Delta_H, theta and

sigma bands in the S2 stage than for the other stages. The sigma band had lower A-AMI for the ELD subjects compared to the MA in the NREM stages. In an earlier study, the regularity measure, sample entropy of EEG was found to correlate with power in the (12-20 Hz) spectral band in sleep. The higher the power of this band, the greater the sample entropy and the lower the regularity of the signal (Bruce et. al., 2009). In the present context, the lower A-AMI of the EEG points to reduced correlations at longer lags of the EEG for the elderly subjects in the S2 and S3 states and hence a greater presence of faster spectral components in sleep of the elderly.

The surrogate data analysis was carried out to check for the presence of correlations in the EEG during sleep that may not be completely captured by a linear approach. Surrogate data analysis is a much advocated method to distinguish nonlinear behavior in EEG analysis. Our findings in this case resemble those in a larger study by Shen and others (2003) where EEG data in NREM stage 2 predominantly exhibited nonlinear behavior. We observed that most of the EEG segments that we analyzed exhibited linear interdependencies. This was especially true for W and REM states. The ELD group had fewer NREM epochs that passed the test for nonlinear correlations in comparison to the MA group. In most studies, significance is calculated as a z-score between the observed nonlinear parameter for the original data and the mean and standard deviation of the same parameter computed for an ensemble of surrogates. However, this approach implicitly assumes the normality of the distribution of the estimated parameters for the set of surrogates. Another method would be to determine if a single parameter, for example, the mean value of the MI estimated over a certain period or the maximum MI value for the signals, was greater than the respective single parameter values for all of the surrogate pairs. Here, we utilize a more conservative approach by including the MI values at each time lag in addition to the single parameter of interest, the average CMI, in the decision to detect nonlinear interdependency. Some of the other methods mentioned above may have resulted in more of the segments being accepted as exhibiting nonlinear interdependence. Between the two age groups, there was a slightly higher occurrence of segments with nonlinear interdependencies for the MA group in the NREM stage and for the ELD group in the REM stage. However, the low CMI values observed among the EEG segments from the ELD caused failure to reject the hypothesis of independence to a greater proportion in comparison to signals from the MA group. Several authors have reported on the nonlinear nature of sleep EEG (Pereda et al, 2001; Fell et al., 1996) and it is generally accepted that both linear and nonlinear features are exhibited by EEG during sleep. However, in a finite data analysis such as ours, the nature of the data may be dynamically changing with the chosen time resolution. This makes MI based analysis a valuable tool in EEG signal analysis where linear and nonlinear dynamics may coexist or be expressed independent of each other.

A crucial point to consider in the estimation of connectivity measures from EEG signals is the bias introduced by effects of volume conduction and the reference electrode in the EEG recording (Nunez et al., 1997; Stam et al., 2007). In this study, the signals were recorded referenced to the mastoids; a procedure usually followed in sleep EEG recordings. An earlier report by Duckrow and Zaveri (2005) compared the intrahemispheric coherence profiles of slow wave sleep obtained from bipolar and common reference derivations. Despite certain topographic differences, common coherence peaks were obtained involving the central regions with respect to anterior or posterior comparisons in both derivations. This would mean that with respect to the central regions, the inter-hemispheric coherence would still be apparent if the signals were referenced to another derivation. However the nature of intra-hemispheric interdependence during sleep and topographic changes with respect to regions other than the central, due to progression of age, are yet to be investigated.

While sleep efficiency and delta band power parameters based on whole night hypnograms exhibit a declining trend for aging subjects, the present analysis shows significant differences between interdependence of central cortical signals in specific sleep stages of two age groups- healthy middle aged and elderly. In the sense that the amplitude based parameters reflect the macroscopic changes in sleep in the elderly in comparison to younger subjects, analyses such as ours provide an answer to whether inherent differences in dynamics are present during typical sleep between age groups. Our findings suggest lowered information transmission in ELD subjects during sleep stages than their younger counterparts. This behavior was also reflected in the different spectral bands, especially the delta, theta and sigma bands. The predictability of the EEG signal based on broad band analysis showed strong variation with sleep stage. The predictability of the REM state in elderly subjects was lower than that for middle aged subjects indicating a more irregular signal in the REM state of the elderly. However it was the sigma band AMI that exhibited lower values in sleep stages of ELD subjects in comparison to the MA group. Hence, while delta band EEG has been known to exhibit reduced power in slow wave sleep with advancing age (Carrier et. al., 2001) we demonstrated the differences in the faster spectral content of the EEG. The physiological implications of our findings relate to the modulation of information transfer between neural circuits involved in generation of the EEG rhythms and how age affects this information transmission between cortical regions during sleep. The reduction of interdependence in the sleep stages of elderly subjects may be due to attenuation of the synchronization in the neuronal activities of spatially separated regions. This may be linked to high levels of activation in sleep as that in waking states and may be a factor affecting sleep quality of elderly subjects.

Acknowledgments

The authors gratefully acknowledge the assistance of the Sleep Heart Health Study (SHHS), which provided the polysomnograms for this study. This paper represents the work of the authors and not the SHHS. This work was supported by National Heart, Lung and Blood Institute cooperative agreements U01HL53940 (University of Washington), U01HL53941 (Boston University), U01HL53938 (University of Arizona), U01HL53916 (University of California, Davis), U01HL53934 (University of Minnesota), U01HL53931 (New York University), U01HL53937 and U01HL64360 (Johns Hopkins University), U01HL63463 (Case Western Reserve University), and U01HL63429 (Missouri Breaks Research).

Sleep Heart Health Study (SHHS) acknowledges the Atherosclerosis Risk in Communities Study (ARIC), the Cardiovascular Health Study (CHS), the Framingham Heart Study (FHS), the Cornell/Mt. Sinai Worksite and Hypertension Studies, the Strong Heart Study (SHS), the Tucson Epidemiologic Study of Airways Obstructive Diseases (TES) and the Tucson Health and Environment Study (H&E) for allowing their cohort members to be part of the SHHS and for permitting data acquired by them to be used in the study. SHHS is particularly grateful to the members of these cohorts who agreed to participate in SHHS as well. SHHS further recognizes all of the investigators and staff who have contributed to its success. A list of SHHS investigators, staff and their participating institutions is available on the SHHS website, www.jhucct.com/shhs. The opinions expressed in the paper are those of the author(s) and do not necessarily reflect the views of the IHS.

This study was supported in part by a grant from the Kentucky Science and Engineering Foundation as per Grant Agreement #KSEF-148-502-05-138 with the Kentucky Science and Technology Corporation. This study was also supported in part by grant AG029304 from the National Institutes of Health.

The authors are grateful to Dr. Richard Kryscio for discussions regarding statistical analysis.

This work was supported by the National Institutes of Health and the Kentucky Science and Engineering Foundation.

References

Abarbanel HDI, Brown R, Sidorowich JJ, Tsimring L Sh. The analysis of observed chaotic data in physical systems. Rev. Mod. Phys 1993;65:1331–92.

Abásolo D, Escudero J, Hornero R, Gómez C, Espino P. Approximate entropy and auto mutual information analysis of the electroencephalogram in Alzheimer's disease patients. Med Biol Eng Comput 2008;46:1019–1028. [PubMed: 18784948]

Acharya RU, Faust O, Kannanthal N, Chua T, Laxminarayan S. Non-linear analysis of EEG signals at various sleep stages. Comp Methods and Pgs Biomed 2005;80:37–45.

Achermann P, Borbély AA. Low-frequency (<1 Hz) oscillations in the human sleep electroencephalogram. Neuroscience 1997;81(1):213–222. [PubMed: 9300413]

Armitage R, Roffwarg HP. Distribution of period-analyzed delta activity during sleep. Sleep 1992;15(6):556–561. [PubMed: 1475571]

Bruce EN, Bruce MC, Vennelaganti S. Sample entropy tracks changes in EEG power spectrum with sleep state and aging. J. Clin. Neurophysiol 2009;26(4):257–266. [PubMed: 19590434]

Burioka N, Miyata M, Cornélissen G, Halberg F, Takeshima T, Kaplan DT, Suyama H, et al. Approximate entropy in the electroencephalogram during wake and sleep. Clin EEG Neurosci 2005;36(1):21–24. [PubMed: 15683194]

Campbell IG, Higgins M, Darchia N, Feinberg I. Homeostatic behavior of fast fourier transform power in very low frequency non-rapid eye movement human electroencephalogram. Neuroscience 2006;140:1395–1399. [PubMed: 16631313]

Cantero JL, Atienza M, Salas RM. Human alpha oscillations in wakefulness, drowsiness period, and REM sleep: different electroencephalographic phenomena within the alpha band. Neurophysiol. Clin 2002;32:54–71. [PubMed: 11915486]

Carrier J, Land S, Buysse DJ, Kupfer DJ, Monk TH. The effects of age and gender on sleep EEG power spectral density in the middle years of life (ages 20-60 years old). Psychophysiol 2001;38:232–242.

Cellucci CJ, Albano AM, Rapp PE. Statistical validation of mutual information calculations: comparison of alternative numerical algorithms. Phys. Rev. E 2005;71:066208.

Corsi-Cabrera M, Guevara MA, Del Rio-Portilla Y, Arce C, Villanueva-Hernandez Y. EEG bands during wakefulness, slow-wave and paradoxical sleep as a result of principle component analysis in man. Sleep 2000;23:1–7.

Darchia N, Campbell IG, Tan X, Feinberg I. Kinetics of NREM delta EEG power density across NREM periods depends on age and delta band designation. Sleep 2007;30(1):71–79. [PubMed: 17310867]

David O, Cosmelli D, Friston KJ. Evaluation of different measures of connectivity using a neural mass model. Neuro Image 2004:659–673. [PubMed: 14980568]

Dijk DJ, Beersma DG, van den Hoofdakker RH. All night spectral analysis of EEG sleep in young adult and middle-aged male subjects. Neurobiol. Aging 1989;10:677–682. [PubMed: 2628779]

Duckrow RB, Zaveri HP. Coherence of the electroencephalogram during the first sleep cycle. Clin. Neurophysiol 2005;116:1088–1095. [PubMed: 15826849]

Ehlers CE, Kupfer DJ. Effects of age on delta and REM sleep parameters. Electroenceph clin Neurophysiol 1989;72:118–125. [PubMed: 2464482]

Escudero J, Hornero R, Abásolo D. Interpretation of the auto-mutual information rate of decrease in the context of biomedical signal analysis: Application to electroencephalogram recordings. Physiol. Meas 2009;30:187–199. [PubMed: 19147896]

Feinberg I, March JD, Floyd TC, Fein G, Aminoff MJ. Log Amplitude is a linear function of log frequency in NREM sleep EEG of young and elderly normal subjects. Electroencephalogr Clin Neurophysiol 1984;58:158–160. [PubMed: 6204842]

Fell J, Roschke J, Mann K, Schaffner C. Discrimination of sleep stages: a comparison between spectral and nonlinear EEG measures. Electroencephalogr Clin Neurophysiol 1996;98(5):401–410. [PubMed: 8647043]

Ferrara M, De Gennaro L, Curcio G, Cristiani R, Bertini M. Regional differences of the temporal EEG dynamics during the first 30 min of human sleep. Neurosci. Res 2002;44:83–89. [PubMed: 12204296]

Ferri R, Rundo F, Bruni O, Terzano MG, Stam CJ. Dynamics of the EEG slow-wave synchronization during sleep. Clin Neurophysiol 2005;116:2783–2795. [PubMed: 16253553]

Fraser AM, Swinney HL. Independent coordinates for strange attractors from mutual information. Phys. Rev. A 1986;33:1134–1140. [PubMed: 9896728]

Guevara MA, Lorenzo I, Arce C, Ramos J, Corsi-Cabrera M. Inter- and intrahemispheric EEG correlation during sleep and wakefulness. Sleep 1995;18(4):257–265. [PubMed: 7618024]

Jeong J, Gore JC, Peterson BS. Mutual information analysis of the EEG in patients with Alzheimer's disease. Clin. Neurophysiol 2001;112:827–835. [PubMed: 11336898]

Kobayashi T, Madokoro S, Wada Y, Misaki K, Nakagawa H. Human sleep EEG analysis using the correlation dimension. Clin Electroencephalogr 2001;32(3):112–8. [PubMed: 11512374]

Lin CM, Davidson TM, Ancoli-Israel S. Gender Differences in Obstructive Sleep Apnea and Treatment Implications. Sleep Med. Rev 2008;12(6):481–496. [PubMed: 18951050]

Lee J-M, Kim D-J, Kim I-Y, Park KS, Kim SI. Nonlinear-analysis of human sleep EEG using detrended fluctuation analysis. Med. Engg & Phys 2004;26:773–776.

Na SH, Jin S-H, Kim SY. The effects of total sleep deprivation on brain functional organization: Mutual information analysis of waking human EEG. Intl. J Psychophysiol 2006;62(2):238–242.

Na SH, Jin S-H, Kim SY, Ham B-J. EEG in schizophrenic patients: mutual information analysis. Clin. Neurophysiol 2002;113:1954–1960. [PubMed: 12464333]

Nunez PL, Srinivasan R, Westdorp AF, Wijesinghe RS, Tucker DM, Silberstein RB, Cadusch PJ. EEG coherency I: statistics, reference electrode, volume conduction, Laplacians, cortical imaging, and interpretation at multiple scales. Electroenceph. Clin. Neurophysiol 1997;103:499–515. [PubMed: 9402881]

Papana A, Kugiumtzis D. Evaluation of mutual information estimators on nonlinear dynamic systems. *Nonlinear Phenomena in Complex* Systems 2008;11(2):225–232. arXiv:0809.2149v1.

Pardey J, Roberts S, Tarassenko L, Stradling J. A new approach to the analysis of the human sleep/wakefulness continuum. J. Sleep Res 1996;5:201–210. [PubMed: 9065871]

Pereda E, Gamundi A, Nicolau MC, Rial R, González J. Interhemispheric differences in awake and sleep human EEG: a comparison between non-linear and spectral measures. Neurosci Lett 1999;263:37–40. [PubMed: 10218905]

Pereda E, Rial R, Gamundi A, González J. Assessment of changing interdependencies between human electroencephalograms using nonlinear methods. Physica D 2001;148:147–158.

Pereda E, Quian Quiroga R, Bhattacharya J. Nonlinear multivariate analysis of neurophysiological signals. Prog. in Neurobiol 2005;77:1–37.

Pivik RT, Harman K. A reconceptualization of EEG alpha activity as an index of arousal during sleep: all alpha activity is not equal. J. Sleep Res 1995;4:131–137. [PubMed: 10607151]

Quan SF, Howard BV, Iber C, Kiley JP, Nieto FJ, O'Connor GT, Rapoport DM, Redline S, Robbins J, Samet JM, Wahl PW. The Sleep Heart Health Study: design, rationale, and methods. Sleep 1997;20(12):1077–1085. [PubMed: 9493915]

Rechtshaffen, A.; Kales, A. A Manual of Standardized Terminology, Techniques, and Scoring Systems of Sleep Stages of Human Subjects. UCLA Brain Information Service/Brain Research Institute; Los Angeles: 1968.

Redline S, Kirchner HL, Quan SF, Gottlieb DJ, Kapur V, Newman A. The effects of age, sex, ethnicity, and sleep-disordered breathing on sleep architecture. Arch. Intern. Med 2004;164:406–418. [PubMed: 14980992]

Schreiber T, Schmitz A. Surrogate time series. Physica D 2000;142:346–382.

Shen Y, Olbrich E, Achermann P, Meier PF. Dimensional complexity and spectral properties of the human sleep EEG. Clin Neurophysiol 2003;114:199–209. [PubMed: 12559226]

Smith MT, Haythornthwaite JA. How do sleep disturbance and chronic pain inter-relate? Insights from the longitudinal and cognitive-behavioral clinical trials literature. Sleep Med. Rev 2004;8:119–132. [PubMed: 15033151]

Stam CJ, Nolte G, Daffertshofer A. Phase lag index: assessment of functional connectivity from multi channel EEG and MEG with diminished bias from common sources. Human Brain Mapping 2007;28:1178–1193. [PubMed: 17266107]

Steriade M, Amzica F. Slow sleep oscillation, rhythmic K-complexes, and their paroxysmal developments. J. Sleep Res 1998;7(l):30–35. [PubMed: 9682191]

Steriade M. Coherent oscillations and short-term plasticity in corticothalamic networks. Trends in Neurosciences 1999;22(8):337–345. [PubMed: 10407416]

Theiler J, Eubank S, Longtin A, Galdrikian B, Farmer DJ. Testing for nonlinearity in time series: the method of surrogate data. Physica D 1992;58:77–94.

Xu J, Liu Z, Liu R, Yang Q. Information transmission in human cerebral cortex. Physica D 1997;106:363–374.

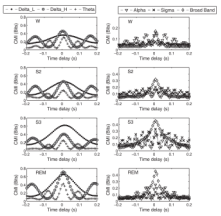

Figure 1.
Typical CMI curves from one middle aged subject as a function of time lag for narrow band and broad band EEG signals. These functions represent the mean of the six segments corresponding to each sleep stage for this particular subject.

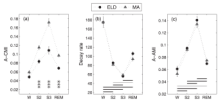

Figure 2.

Broad band EEG analysis: Mean CMI (A-CMI) between C3A2 and C4A1 is on the extreme left (a) and the AMI parameters- decay rate (b) and average AMI (A-AMI) in (c) are plotted across sleep stages. The error bars represent the standard error in the estimated mean of a measure in a particular sleep stage. The asterisks mark the significant (AGEGROUP*STAGE) interactions- *p<0.05, **p<0.005 and ***p<0.0001. In the AMI parameters, the horizontal lines represent the post-hoc results of the significant STAGE effect. Dashed line, p<0.05, thin solid line p<0.005 and thick solid line p<0.0001.

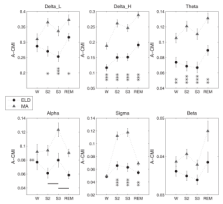

Figure 3.
Average CMI (A-CMI) (Mean ± S.E.) across sleep stages grouped by age for the various spectral bands. Significant differences are marked as, * p<0.05, **p<0.005, ***p<0.0001. In the case of Alpha band, the lines denote the post-hoc results for the STAGE effect when connecting two stages marked along the x-axis. Thick solid line, p<0.0001, thin solid line, p<0.005 and dashed line, p<0.05. Also the significant AGE effect for this band is denoted by the asterisks on the left side inside the plot window.

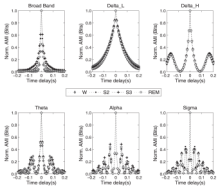

Figure 4.

AMI curves for the broad band and the filtered C3-A2 signal in the different sleep stages as a function of the delay time. The curves shown here were obtained by averaging the AMI function for the individual segments (6) of each sleep stage in a middle aged subject. The same behavior was observed in all other subjects' data.

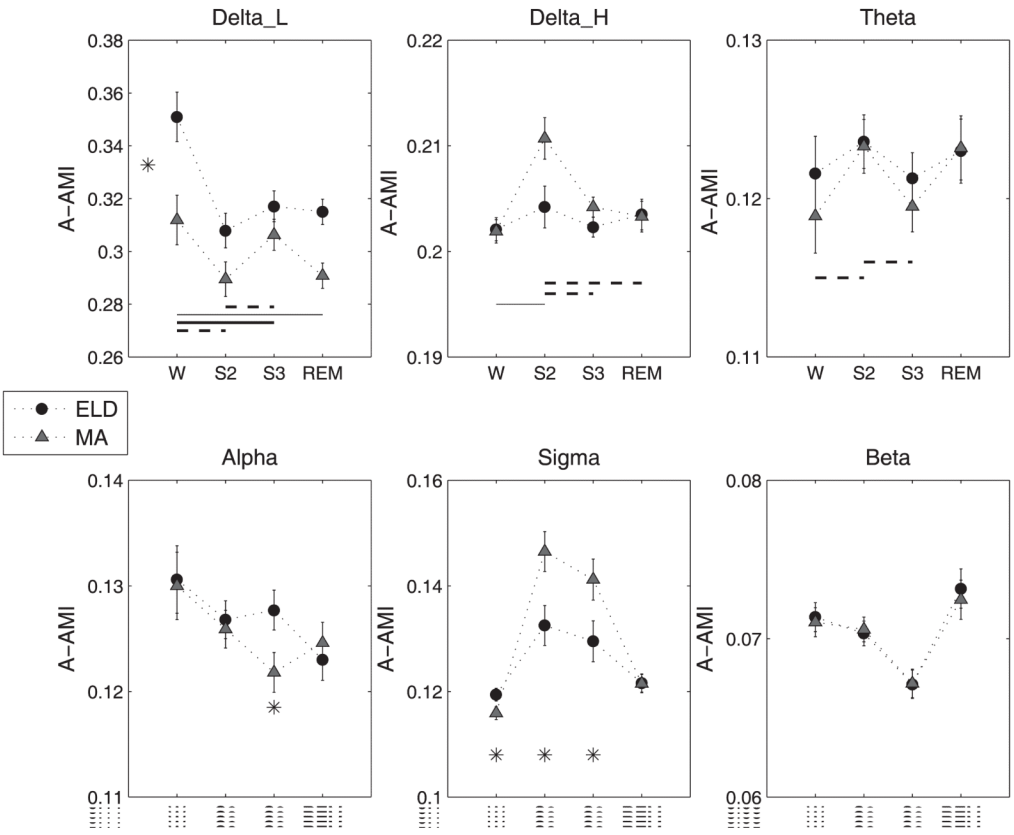

Figure 5.

(Mean ± S.E.) of the A-AMI measure for the spectral bands. The asterisk ($p<0.05$) denotes significant main effect in AGEGROUP when marked between the A-AMI values corresponding to the two groups (Delta_L band). It denotes significant AGEGROUP*STAGE effect when marked below the A-AMI values at specific sleep stages. The lines denote the post-hoc results for the STAGE effect when connecting two stages marked along the x-axis. Thick solid line, $p<0.0001$, thin solid line, $p<0.005$ and dashed line, $p<0.05$.

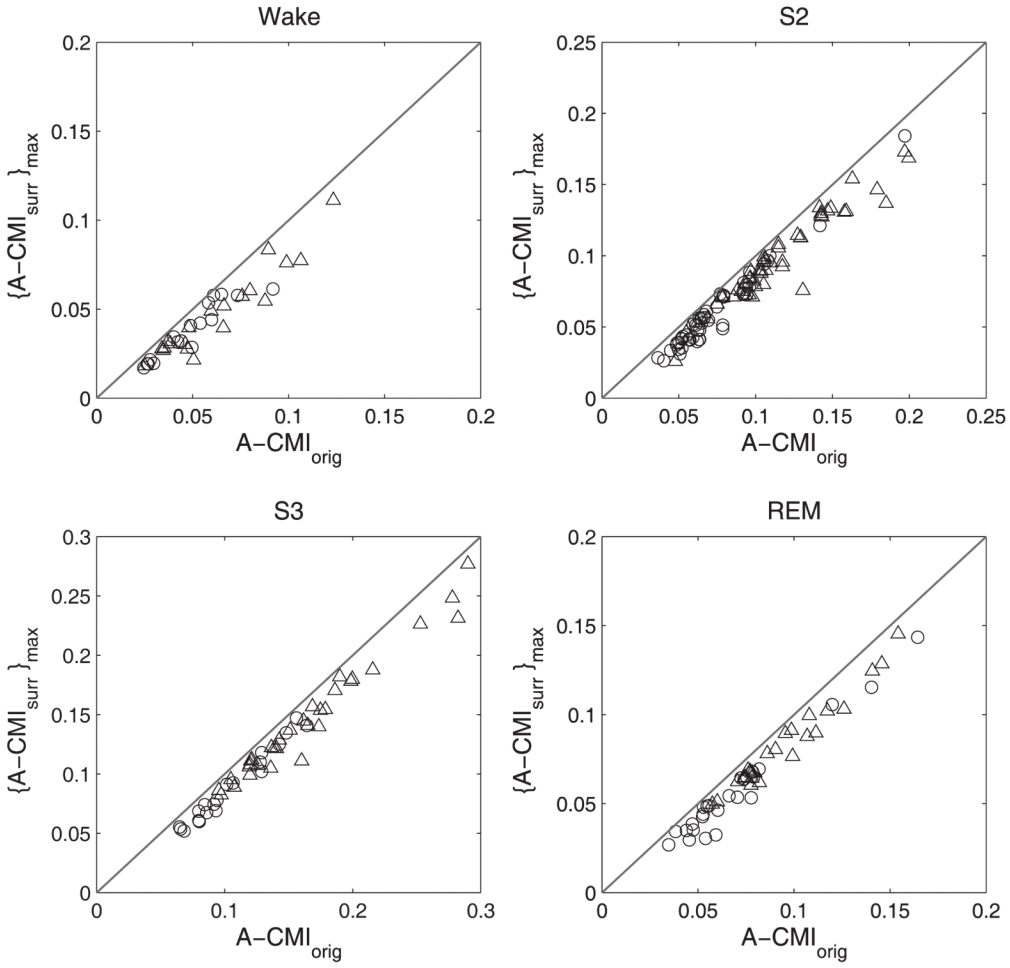

Figure 6.

Results of the surrogate data analysis applied to EEG segments from ELD (circles) and MA (triangles) subjects. The line of identity represents the equality between the average CMI for the EEG segments [A-CMI_{orig}] and the maximum value from the ensemble of the average CMI calculated for the surrogate pairs [{A-CMI_{surr}}$_{max}$].